



## King's Research Portal

DOI:

[10.1016/j.cortex.2018.08.030](https://doi.org/10.1016/j.cortex.2018.08.030)

*Document Version*

Peer reviewed version

[Link to publication record in King's Research Portal](#)

*Citation for published version (APA):*

Karolis, V. R., Grinyaev, M., Epure, A., Tsoy, V., Du Rietz, E., Banissy, M. J., Cappelletti, M., & Kovas, Y. (2018). Probing the Architecture of Visual Number Sense with Parietal tRNS. *Cortex*.  
<https://doi.org/10.1016/j.cortex.2018.08.030>

### **Citing this paper**

Please note that where the full-text provided on King's Research Portal is the Author Accepted Manuscript or Post-Print version this may differ from the final Published version. If citing, it is advised that you check and use the publisher's definitive version for pagination, volume/issue, and date of publication details. And where the final published version is provided on the Research Portal, if citing you are again advised to check the publisher's website for any subsequent corrections.

### **General rights**

Copyright and moral rights for the publications made accessible in the Research Portal are retained by the authors and/or other copyright owners and it is a condition of accessing publications that users recognize and abide by the legal requirements associated with these rights.

- Users may download and print one copy of any publication from the Research Portal for the purpose of private study or research.
- You may not further distribute the material or use it for any profit-making activity or commercial gain
- You may freely distribute the URL identifying the publication in the Research Portal

### **Take down policy**

If you believe that this document breaches copyright please contact [librarypure@kcl.ac.uk](mailto:librarypure@kcl.ac.uk) providing details, and we will remove access to the work immediately and investigate your claim.

# Accepted Manuscript

Probing the Architecture of Visual Number Sense with Parietal tRNS

V.R. Karolis, M. Grinyaev, A. Epure, V. Tsoy, E. Du Rietz, M.J. Banissy, M. Cappelletti, Y. Kovas



PII: S0010-9452(18)30282-X

DOI: [10.1016/j.cortex.2018.08.030](https://doi.org/10.1016/j.cortex.2018.08.030)

Reference: CORTEX 2402

To appear in: *Cortex*

Received Date: 25 November 2017

Revised Date: 12 May 2018

Accepted Date: 30 August 2018

Please cite this article as: Karolis VR, Grinyaev M, Epure A, Tsoy V, Du Rietz E, Banissy MJ, Cappelletti M, Kovas Y, Probing the Architecture of Visual Number Sense with Parietal tRNS, *CORTEX* (2018), doi: 10.1016/j.cortex.2018.08.030.

This is a PDF file of an unedited manuscript that has been accepted for publication. As a service to our customers we are providing this early version of the manuscript. The manuscript will undergo copyediting, typesetting, and review of the resulting proof before it is published in its final form. Please note that during the production process errors may be discovered which could affect the content, and all legal disclaimers that apply to the journal pertain.

# PROBING THE ARCHITECTURE OF VISUAL NUMBER SENSE WITH PARIETAL tRNS.

Karolis, V.R.<sup>1,2,\*</sup>, Grinyaev, M.<sup>3</sup>, Epure, A.<sup>4</sup>, Tsoy, V.<sup>3</sup>, Du Rietz, E.<sup>5</sup>, Banissy, M.J.<sup>6</sup>, Cappelletti, M.<sup>6,7,#</sup>, & Kovas, Y.<sup>3,6,#</sup>

<sup>1</sup> Department of Psychosis Studies, Institute of Psychiatry, Psychology, and Neuroscience, King's College London, UK

<sup>2</sup> Frontlab, Institut du Cerveau et de la Moelle épinière (ICM), Hôpital de la Salpêtrière, France

<sup>3</sup> International Centre for Research in Human Development, Tomsk State University, Russia.

<sup>4</sup> Department of Experimental Psychology University of Oxford, UK

<sup>5</sup> MRC Social, Genetic and Developmental Psychiatry Centre, Institute of Psychiatry, Psychology and Neuroscience, King's College London, UK.

<sup>6</sup> Department of Psychology, Goldsmiths, University of London, UK.

<sup>7</sup> Institute of Cognitive Neuroscience, University College London, UK.

# - these authors contributed equally

\* - corresponding author

Please address correspondence to: V. Karolis, [slava.karolis@kcl.ac.uk](mailto:slava.karolis@kcl.ac.uk), Department of Psychosis Studies, 16 De Crespigny Park, Camberwell, London, UK, SE5 8AF

**Keywords:** visual number sense, number code, weighted integration, intraparietal cortex, superior parietal cortex

**ABSTRACT**

Theoretical accounts of the visual number sense (VNS), i.e., an ability to discriminate approximate numerosities, remain controversial. A proposal that the VNS represents a process of numerosity extraction, leading to an abstract number representation in the brain, has been challenged by the view that the VNS is non-numerical in its essence and amounts to a weighted integration of continuous magnitude features that typically change with numerosity. In the present study, using two-alternative forced-choice paradigm, we aimed to distinguish between these proposals by probing brain areas implicated in the VSN with transcranial random noise stimulation (tRNS). We generated predictions for the stimulation-related changes in behavioural performance which would be compatible with alternative mechanisms proposed for the VSN. First, we investigated whether the superior parietal (SP) area hosts a numerosity code or whether its function is to modulate weighting of continuous stimulus features. We predicted that stimulation may affect the VNS precision if the SP role is representational, and that it may affect decision threshold if its role is modulatory. Second, we investigated whether the intra-parietal (IP) area hosts a numerosity code independently of codes for continuous stimulus features, or whether their representations overlap. If the numerosity code is independent, we predicted that IP stimulation may improve the VNS but not continuous magnitude judgements. Our results were consistent with the hypotheses of a modulatory role of the SP and of the independence of the numerosity code in the IP, whereby suggesting that VNS is an emergent abstract property based on continuous magnitude statistics.

## 1. Introduction

Extracting an approximate numerosity of a set from a visual scene, for instance the number of dots (aka visual number sense, VNS), is a primitive, cross-species and cross-cultural ability (Dehaene, Izard, Spelke, & Pica, 2008; Nieder, Freedman, & Miller, 2002). VNS tasks are widely used to assess basic magnitude skills (Davidse, de Jong, Shaul, & Bus, 2014; Halberda & Feigenson, 2008; Iuculano, Tang, Hall, & Butterworth, 2008), with some researchers arguing that the VNS represents a foundational ability for developing arithmetical competence (Halberda, Mazocco, & Feigenson, 2008; Jordan, Glutting, & Ramineni, 2010; Piazza et al., 2010; Tibber et al., 2013). Different theoretical accounts of the VNS have been put forward, although there is currently no agreement on the nature of the cognitive mechanisms supporting this ability.

One of these accounts, the Approximate Number System (ANS) model proposes a three-stage hierarchical process of numerosity extraction (Dehaene & Changeux, 1993; Verguts & Fias, 2004). Firstly, the items to be enumerated are converted into an object location map by normalising continuous magnitude features that confound numerosity estimate (e.g., the area of individual items). The second processing layer pools together (summates) the output of the object location map. In the final stage, the results of the summation are converted into a number-selective code.

The ANS model, however, has been challenged by the suggestion that stimulus numerosity can be obtained without item enumeration through a weighted integration of continuous magnitude features (Gebuis, Kadosh, & Gevers, 2016; Gebuis & Reynvoet, 2012; Karolis & Butterworth, 2016; Stoianov & Zorzi, 2012). Several studies demonstrated that

systematic manipulations of continuous magnitudes can bias numerosity judgements (Gebuis & Reynvoet, 2012; Dakin, Tibber, Greenwood, Kingdom, & Morgan, 2011; Tibber, Greenwood, & Dakin, 2012). This has been taken to suggest that no abstract numerosity representation is constructed from perceptual magnitudes and that the metric for approximate number relies on the metric for continuous magnitudes (Gebuis, Kadosh, & Gevers, 2016; Dakin et al., 2011). A compromise between the ANS and the weighted-integration hypotheses has also been proposed: an abstract 'read-out' of approximate numerosity may exist in the brain as an emergent property of the integration of continuous magnitudes (Karolis & Butterworth, 2016; Stoianov & Zorzi, 2012).

One way to distinguish between these hypotheses is to examine the role of the brain regions known to contribute to numerosity processing. Thus, the ANS architecture is consistent with the evidence of two types of coding for magnitudes in the primate brain (Nieder, 2016; Roitman, Brannon, & Platt, 2012). Firstly, the summation code (Stage Two) may be reflected in the observed activity in the lateral intraparietal area, a likely homologue of the human superior parietal lobule (SPL) (Koyama et al., 2004; Sereno, Pitzalis, & Martinez, 2001), which increases incrementally with the number of items presented in a display (Roitman, Brannon, & Platt, 2007). Secondly, the number-selective code (Stage Three), may be implemented by neurons in the intraparietal sulcus (IPS), which act as number-selective filters such that their tuning curves are centred on preferred magnitudes (Nieder & Miller, 2004). Evidence for the two types of coding in the SPL and IPS has also been demonstrated in fMRI of human participants (Harvey, Klein, Petridou, & Dumoulin, 2013; Piazza, Izard, Pinel, Le Bihan, & Dehaene, 2004; Santens, Roggeman, Fias, & Verguts, 2010).

In support of weighted integration hypothesis, other brain studies have shown that the activity in the IPS is modulated by the presentation of continuous magnitudes as well as numerosities (Pinel, Piazza, Le Bihan, & Dehaene, 2004; Walsh, 2003). So far the role of the SPL in the process of weighted magnitude integration remains, however, unspecified. Its generic function has been described as ‘priority maps’, incorporating, as a part of dorsal attentional network (Corbetta & Shulman, 2002), the top-down feedback in order to modulate bottom-up visual information in accordance with task demands (Bisley & Goldberg, 2010). The SPL could therefore implement a modulation of the weights applied to continuous magnitudes rather than summation coding for numbers.

In the present study, we aimed at differentiating among the alternative hypotheses on the VNS architecture by probing neural substrate for cognitive mechanisms implicated in the VSN with transcranial random noise stimulation (tRNS). Specifically, we addressed two research questions. The first was whether the superior parietal area plays a representational or modulatory role in the VNS; that is, whether it implements a type of numerosity code, as proposed by ANS model, or whether instead it implements weights for continuous stimulus features. The second question was whether the intraparietal region represents a numerosity ‘read-out’ independent of continuous magnitudes or whether their metrics overlap.

## **1. 1. This study**

In the two-alternative forced-choice paradigm (2AFC) task, participants chose between numerical magnitudes of two stimuli that contained equally sized dots scattered over mismatched areas (Dakin et al., 2011) (Figure 1A). One of the stimuli, the “reference”,

maintained constant stimulus area and spatial frequency of dots (and hence numerosity) over the entire block of trials; in the other stimulus, the “test”, the stimulus area remained constant but the dot spatial frequency varied from trial to trial.

Here tRNS was used instrumentally in order to differentiate between alternative hypotheses. tRNS has been shown to increase excitability of stimulated neuronal population, likely to be mediated by potentiation of sodium voltage-gated channels (Chaieb, Antal, & Paulus, 2015) and arguably is independent of gyrus folding (Terney, Chaieb, Moliadze, Antal, & Paulus, 2008). Increased excitability of a brain region in response to a stimulus is known as a response gain, i.e., a (proportional) increase of a response rate of neuronal populations (Reynolds & Heeger, 2009). We hypothesised that this may lead to two possible effects on behavioural performance. If a brain area implements a type of numerosity code, a tRNS-evoked response gain may result in a better discriminability between two stimuli (Carrasco, Ling & Read, 2004; Brezis, Bronfman, Jacoby, Lavidor, & Usher, 2016). This can be measured as a steeper slope of a psychophysical function that fits the probability of choosing a test stimulus in reference to a standard (Figure 1B). In contrast, if a brain area plays a modulatory role in the VNS, then the response gain is elicited in neuronal populations that implement magnitudes' weighting rather than their representations per se. A systematic modulation on weights may then result in a change of the decision threshold, a contrast gain (Carrasco, Ling & Read, 2004; Reynolds & Heeger, 2009). This can be measured as a horizontal shift of the psychophysical function (Figure 1 – C).

The above effects should be distinguished from an involuntary attentional enhancement in the processing of low-level stimulus features and/or the modulation of stimulus salience

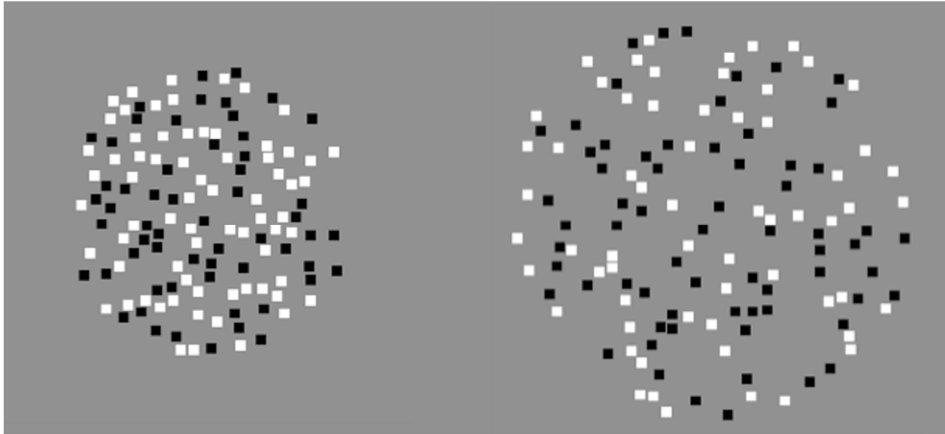


(Kastner & Ungerleider, 2001; Keitel, Andersen, Quigley, & Muller, 2012), typically associated with the function of the ventral attentional network (Corbetta & Shulman, 2000) and which may also result in a better precision and/or in an effect on the decision threshold (Reynolds & Heeger, 2009). In order to rule out this possibility, we administered two control tasks requiring continuous magnitude judgements – spatial frequency (density) and motion coherence. The presentation parameters of these tasks, especially the density task, closely matched those of the numerosity task. We hypothesised that performance in these control tasks may be equally affected if stimulation modulates the processing of low-level stimulus features.

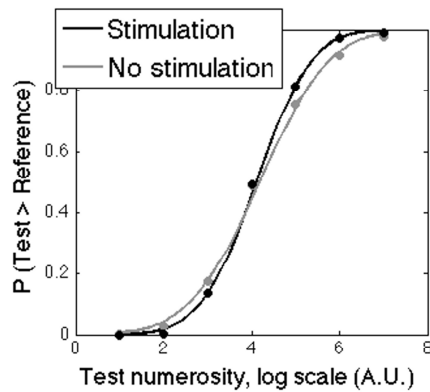
Abundant evidence accentuates the role of brain networks in cognitive functioning (e.g., Bressler & Menon, 2010) and modelling evidence suggests that electrical stimulation may cause network re-configuration in addition to altering activity in a stimulated region (Polania, Paulus, Antal, & Nitsche, 2011). Consequently, in contrast to anatomically defined SPL and IPS and in the absence of precise localisation for the stimulation-dependent activity changes, we will use the terms ‘SP’ and ‘IP’ as shortcuts to denominate functional systems which may also include regions which are anatomically or functionally connected to stimulation loci defined using the EEG 10-20 system.

To summarise, we predicted that tRNS stimulation may improve the VNS precision if the SP plays a representational role in the VNS, and may affect the decision criterion if its role is instead modulatory. We also predicted that if the IP represents a ‘read-out’ of numerosity independent of continuous magnitudes, then stimulating this region may improve the VNS precision in numerosity independently of continuous magnitude judgements.

(A)



(B)



(C)

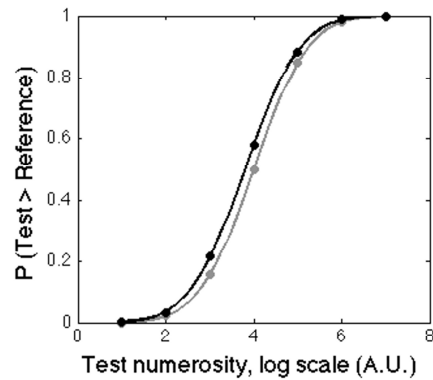


**Figure 1. Experimental stimuli and predictions of the stimulation effects. (A) Example of a stimuli pair. The areas covered by the dot stimuli were always mismatched to prevent making judgments only on the basis of one task-relevant stimulus feature. Dot spatial frequency (= the number of dots) of one stimulus varied from trial to trial, whereas the other maintained constant magnitude characteristics. Note that the numerosity of a stimulus in the log space (natural space for visual number) can be parameterised as a weighted sum of stimulus density  $D$  and area  $A$ , i.e.,  $W_d \cdot D + W_a \cdot A$ . (B) Predictions for the ANS model. A steeper slope following stimulation is due to a response gain in stimulated neuronal populations. (C) Predictions for the weighted integration model. The horizontal shift in the fitting function occurs if weights associated with magnitude of one stimulus would increase/decrease.**

## **2. Method**

### **2.1. Participants**

An opportunistic sample of 54 healthy, stimulation compatible (Wassermann, 1998) participants was enrolled on the University campus. All participants provided informed written consent to participate in the study ( $M = 20.6$  years,  $SD = 2$  years, 37 females and 17 males). The study was approved by Ethics Committee for Interdisciplinary Investigations (Tomsk State University, Russia).

### **2.2. Apparatus**

The experiment was conducted in a darkened room with participants' head movements restricted by a chinrest located 60 cm in front of a 19-in LCD monitor (1440 by 900 pixels, pixel size .265 mm). The midline of the eyesight approximately coincided with the centre of the monitor. Stimuli were presented using Cogent toolbox (UCL Institute of Neurology) for Matlab (Mathworks Inc). Random noise stimulation (0.1 – 640 Hz, 2.0 mA peak-to-peak with zero-mean offset) with fade-in and fade-out phase lasting 15 seconds was delivered for 20 minutes. A NeuroConn DC Brain Stimulator Plus unit was used (Rogue Resolutions, Wales, UK), and the current was delivered through a pair of 3 cm x 3 cm electrodes. No saline-soaked sponges were used, and electrodes were applied directly to the scalp and fixated using an elastic EEG cap. An EEG gel was used to reduce skin impedance (van der Groen & Wenderoth, 2016)

### **2.3. Experimental task**

A two-alternative forced-choice numerosity task (N task) was used, whereby participants were presented with two circular clouds of white and black, equally-sized square dot stimuli ( $0.12^\circ$  of visual angle at the viewing distance of 60 cm) displayed on a grey background for 250 ms (Figure 1A) (Dakin et al., 2011). Participants judged which cloud contained the larger number of dots under no time pressure within a maximum response time of 2000 ms from the stimulus onset. The stimuli were presented to the left and right of central fixation, with  $7.6^\circ$  separation between their centres. The positions of the dots within each stimulus cloud was randomly generated, ensuring there was no overlap between them. A fixation cross was presented 500 ms before the stimuli and disappeared at the moment of their presentation. Participants were asked to maintain their eye gaze on the fixation cross during a trial. Participants responded unimanually by pressing the left or right button on keyboard. In order to maintain a between- and within-subject equality in the duration of an experimental session, the length of each trial was fixed, with the next trial starting after 2000 ms from the presentation of a stimulus in a previous trial.

For each pair of stimuli, one was the Reference stimulus that always contained 128 dots, and the other was the Test stimulus, for which the number of dots varied from trial to trial. The left-right order of presentations for the Test and Reference stimuli was selected randomly. There were 7 levels for the Test stimulus: 64, 82, 102, 128, 164, 204, or 256 dots, presented in a randomised order. Each level was presented 21 times per each block. In order to ensure that statistics for each level of stimuli were based on the same number of trials, the trials where participants failed to respond within the allowed response window were repeated later in the experiment, with their position in the trial order selected at random. The areas covered by the

Reference and Test stimuli clouds were fixed over the length of an entire experimental block but were always mismatched, with the diameter of one cloud being small ( $4^\circ$  of visual angle) and the other large ( $5.7^\circ$  of visual angle). The task consisted of two experimental blocks. In one block, the area of the Test stimulus was smaller than the area of the Reference stimulus ('Small Test/Large Reference' condition); in the other, the area of the Test stimulus was larger than the area of the Reference stimulus ('Large Test/Small Reference' condition). The mismatch of the areas coupled with varying dot density in the Test stimulus ensured that the N task meets a minimal criterion for a numerosity task; that is, stimulus magnitudes could not be accurately determined over the run of trials using one stimulus dimension only (cloud area or dot density).

#### **2.4. Density and motion coherence tasks**

Two control tasks were also administered. One task, a density discrimination task (D task) mimicked the design of the N task except that participants selected a set with greater dot density, i.e., the smaller average distance between pairs of dot stimuli. The D task shared one task-relevant magnitude with the N task and making judgements on this magnitude was sufficient to perform in the task. The other task, a motion coherence task (C task), required judgments of magnitudes unfolding in the temporal domain. Participants observed clouds of moving dots, whose trajectories were composed of both random and deterministic components, and judged which stimulus contained a more orderly/less random motion pattern. The C task shared a two-dimensional stimulus structure with the N task while maintaining a 3-way dissimilarity in feature types (random and deterministic components vs. density and area), their relations (ratio "random/deterministic" vs. product "density x area"), and temporal

structure (temporally unfolding vs. instantaneous). Presentation parameters in both control tasks were closely matched to the N task, apart from stimulus presentation window in the C task, which was extended up to 2000 ms or the time of participant's response, whichever occurred earlier. Like the N task, the area of the Test and Reference stimuli, non-informative for the performance in these tasks, was fixed but it was always mismatched; the task-relevant dimension was fixed for the Reference stimulus and was varying from trial to trial for the Test stimulus.

In the D task, the Reference stimulus always contained 128 dots and the Test stimulus contained 50, 64, 80, 100, 128, 160, or 200 % of Reference density. In the C task, participants viewed two sets of 128 moving dot stimuli, containing both non-random and random components in their motion. The direction of the motion non-random component was upward or downward, selected at random. The direction of the motion random component was obtained by randomly sampling an angle of deviation from a notional vertical line. The lengths of non-random ( $L_{\text{nrnd}}$ ) and random ( $L_{\text{rand}}$ ) components were set using formula:  $k (L_{\text{nrnd}}^2 + L_{\text{rand}}^2) = 1.7^\circ/\text{sec}$ . The ratio between  $L_{\text{nrnd}}$  and  $L_{\text{rand}}$  determined stimulus levels. The scaling parameter  $k$ , found by simulations, was used to ensure that the average length of the dot path ('speed') did not differ between stimulus levels and could not be used as an additional cue for magnitude judgments. A pilot study indicated that subjective scale was not linear (linear scale characterises a standard variant of motion coherence task - e.g., Roitman & Shadlen, 2002) and were more likely to scale with the ratio between standard deviations of left-right and upward-downward displacements. Accordingly, ratios between random and non-random components

defining the Test stimulus levels were chosen as 0.05, 0.23, 0.35, 0.43, 0.50, 0.55 and 0.60. The mid-value in the sequence (0.43) was used as a magnitude for the Reference stimulus.

## 2.5. Procedure

Participants' recruitment and data collection were administered by researchers who were unaware of the specific hypotheses of the study. Each participant was assigned to one of the three groups, referred to as the superior parietal (SP), the intraparietal (IP), and the control motor (CM) groups. Based on the EEG 10-20 system, the SP group received stimulation to regions defined as half-way between PZ and P3 on the left side and half-way between PZ and P4 on the right side. Participants in the IP group received stimulation bilaterally to parietal areas corresponding to P3 and P4; in the CM group - to areas C3 and C4. The performance of CM group was used as a quantitative baseline for the changes elicited by tRNS in parietal regions. Given that motor areas are not known to be involved in a specialised cognitive processing of visual magnitudes, their stimulation also provides a control for spatially indiscriminate effects, e.g., stimulation factor affecting performance irrespective of the stimulation locus.

Prior to sitting the main experimental session, participants attended a pre-stimulation session designed to stabilise task performances (DeWind & Brannon, 2012) and to familiarise participants with the tasks. The pre-stimulation session took place on a separate day, within a week of the main experimental session, and was its abridged version, with each task consisting of 16 trials for each level of the test stimulus and two blocks, 'Small Test/Large Reference' and 'Large Test/Small Reference'. The data from the pre-stimulation session were not analysed and

therefore they had no effect on the participant's assignment to a group which was done prior to the pre-stimulation session.

The main experimental session started with a short practice session of 20 trials per task, which were not included in the data analysis. All three tasks were then administered twice, before and following brain stimulation, hereafter – the Before and After sessions. The order of the tasks in the Before session was repeated in the After session, but it was fully counter-balanced across participants. On completing the Before session, participants received 20 minutes of stimulation. Participants continued performing the tasks after 13 minutes from the start of the stimulation.

## **2.6. Data analysis**

### **2.6.1. Performance measures**

The design of each task contained stimulation Group as a between-participant factor (SP vs. CM vs. IP), and 3 within-participant factors: Session (Before vs. After stimulation), Test stimulus Area ('Small Test Area/Large Reference Area' vs. 'Large Test Area/Small Reference Area'), and 7 levels of the Test stimulus intensity. To fit the data, standard procedures of psychophysical fitting were used as follows. First, for each participant, a proportion of Test > Reference responses was calculated for each intensity level of the Test stimulus for each combination of the other factors. Second, the calculated proportions were fitted using a cumulative Gaussian function, which rendered two standard statistics: the slope (Gaussian standard deviation) and the threshold (Gaussian mean). Four values were obtained per each participant (2 Sessions by 2 Test stimulus Areas) for each measure. The estimated value for the



slope was divided by a square root of 2 to obtain an estimate of the Weber Fraction (WF), i.e., the measure of internal variability of magnitude representations, with smaller values of WF signifying a better accuracy. WFs were analysed in log space, as this measure demonstrates the features of a log-normal variable (Lambrechts, Karolis, Garcia, Obende, & Cappelletti, 2013): a) have a positive skew and, critically, b) the (unsigned) changes in WFs would also be positively skewed. In all analyses, a negative change in WF between the Before and After sessions designated a relative improvement in VNS precision. For threshold, a negative value indicated an overestimation of a Test stimulus magnitude; hence a negative change between the Before and After sessions would indicate a contrast gain (relative overestimation) for a Test stimulus. The data were fitted using Psignifit toolbox for Matlab (Frund, Haenel, & Wichmann, 2011).

### 2.6.2. Statistical modelling

To account for the factors associated with the changes in threshold and WF between the Before and After sessions, the linear mixed-effect regression modelling was used in combination with the model comparison procedure. This approach pursued two goals. Firstly, by modelling the effect of confounding factors, both random and fixed, we sought to obtain more accurate and robust estimates of the effects of interest. Secondly, by using the change in threshold and WF in the control tasks as additional predictors, we aimed to either confirm or reject a statistical independence of these changes from the changes in the N task.

Our analyses start with the definition of a benchmark model that characterises the task design. In Wilkinson notation (Wilkinson & Rogers, 1973), this model is:

$$\text{Model 1: } dY = \text{Group} + \text{TestArea} + \text{Group:TestArea} + (\text{TestArea}|\text{Participant}),$$

where  $dY$  stands for the change of a parameter of interest (either WF or threshold) between Before and After sessions; notation  $\text{Group:TestArea}$  stands for an interaction term between two factors and  $(\text{TestArea}|\text{Participant})$  codes for repeated measures via grouping of the Test stimulus area by a random Participant factor.

To pursue Goal 1, Model 1 was contrasted with alternative models, which accounted for possible confounding effects, both fixed and random, of two factors: 1) the baseline performance as measured in the Before session,  $\text{base}_Y$ ; and 2) the change in the un-modelled parameter  $dX$  between Before and After sessions (i.e., the change in WF as a confounding factor for the change in threshold and vice versa). The complete list of evaluated models is presented in Table 1. All models were fitted using Statistics toolbox for Matlab. The model comparison was performed using Bayesian Information Criterion. The independence of the change of the WF and threshold from the change in the same parameters in the control task (Goal 2) was then ascertained by adding these parameters as additional predictors to a best fitting model identified by the above model selection procedure.

**Table 1. List of models compared in the study.**

Model in Wilkinson notation	What is tested
1 $dY = \text{Group} + \text{TestArea} + \text{Group:TestArea} + (\text{TestArea} \text{Participant})$	Benchmark model
2 $dY = \text{Group} + \text{TestArea} + \text{Group:TestArea} +$	Same as 1, but uses performance in the Before session grouped by random Participant to account

$(base\_Y Participant)$	for repeated measures
3 $dY = Group + TestArea + Group:TestArea + base\_Y + (TestArea Participant)$	Same as 1, but adding performance in the Before session as additional factor
4 $dY = Group + TestArea + Group:TestArea + base\_Y + (base\_Y Participant)$	Same as 3, but uses performance in the Before session grouped by random Participant to account for repeated measures
5 $dY = Group + TestArea + Group:TestArea + (dX Participant)$	Same as 1, but uses change in unmodelled parameter (i.e., change in threshold if $dY$ is WF and vice versa) grouped by random Participant to account for repeated measures
6 $dY = Group + TestArea + Group:TestArea + dX + (TestArea Participant)$	Same as 1, but adding change in unmodelled parameter (i.e., change in threshold if $dY$ is WF and vice versa) as additional factor
7 $dY = Group + TestArea + Group:TestArea + dX + (dX Participant)$	Same as 5, but adding change in unmodelled parameter (i.e., change in threshold if $dY$ is WF and vice versa) as additional factor

### 2.6.3. Supplementary data set

As shown in Results section (see below), the performance measures in the N task of the CM group altered between the Before and After sessions. Consequently, we report supplementary data demonstrating that the patterns observed in the CM group do not reflect unexpected and task-specific (see Discussion for details) stimulation effects but are rather typical patterns of performance under no-stimulation condition. The data acquired as a part of a preliminary study comprises performance measures of 18 participants (mean = 23.7, SD = 5.3, 14 females and 4 males) who received sham IP stimulation. The study was approved by Goldsmith Ethical Committee. These supplementary data are not directly comparable to the main experimental dataset as they were collected in a different location and using a different set-up. The study did not include a pre-stimulation session; participants attended the main experimental session only. The sham stimulation consisted of 15 secs stimulation at the

beginning and the end of the 20-minute interval. The electrodes were placed into saline-soaked pads and attached to the head using rubber stripes.

### 3. Results

Measures of performance for all tasks and conditions are plotted in Figure 2.

#### 3.1. Baseline performance

The performance at the baseline was modelled using the benchmark Model 1 using the threshold and WF in the Before session as dependent variables.

No group differences were observed in any task for threshold. For Weber fraction (WF), there were no group differences in the N and D tasks, but there was a significant effect of Group in the C task ( $F(2, 102) = 5.33, p < 0.01$ ), suggesting that performance specifically between the IP and SP groups (planned contrast test:  $F(1, 102) = 10.65, p < .005$ ), was not entirely matched for this task.

Across all groups, there was a significant effect of Test Area on the thresholds in the D and N tasks, ( $F(1, 102) = 54.20, p < 0.001$ , and  $F(1, 102) = 6.73, p = 0.011$ , respectively, see Table 2). In the D task, participants underestimated the magnitude of the Small Test and overestimated the magnitude of the Large Test. The opposite pattern, that is, an underestimation of the Large Test, was observed in the N task. No effect of Test Area was observed in the C task ( $p > .25$ ).

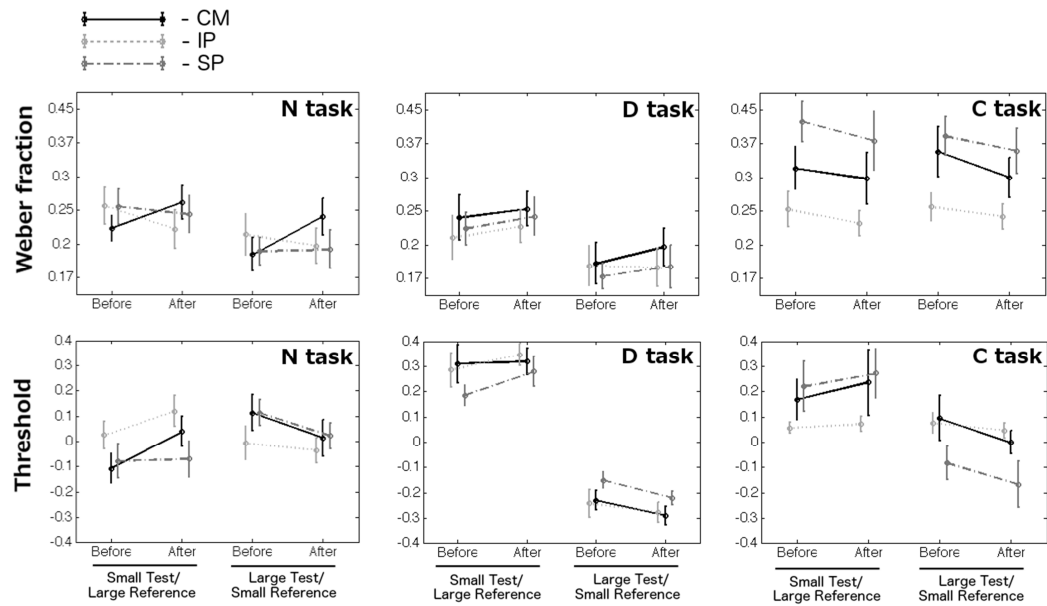


**Figure 2.** Performance measures for all stimulation conditions and groups. Smaller values for the Weber Fraction, plotted on the log scale, imply better precision. For threshold, negative values reflect overestimation of the Test stimulus, positive values its underestimation. Error bars show the standard error of the mean.

**Table 2.** Effects of test stimulus area on baseline threshold. Intercept encodes the threshold value for the Small Test/Large Reference condition. Large Test/Small Reference encodes the difference from Small Test/Large Reference condition. Negative values reflects overestimation (a leftward shift of a psychophysical function) and positive values an underestimation (a rightward shift). The beta associated with Small Test/Large Reference is approximately twice as large as the beta for the in either tasks. This indicates an approximately symmetrical deviation from the point of objective equality for two types of test stimulus. The overestimation/underestimation pattern is opposite for N and D tasks.

<b>D task</b>					
Predictors	beta	CI (Lower/Upper)		t (df =102)	P-value
Intercept	0.28	0.18	0.39	5.47	< 0.001
Large Test/Small Reference	-0.54	-0.68	-0.39	-7.36	< 0.001
<b>N task</b>					
Predictors	beta	CI (Lower Upper)		t (df =102)	P-value
Intercept	-0.12	-0.23	0.00	-2.01	0.048
Large Test/Small Reference	0.22	0.05	0.39	2.59	0.011

### 3.2. Effect of stimulation on the Weber Fraction

#### 3.2.1. N task

Model selection procedure identified Model 4 as a best-fitting model for the N task, suggesting a significant association between the WF change and WF magnitude at baseline. The difference in Bayesian Information Criterion from the benchmark Model 1 was equal to 15.99, implying very strong evidence (Kass & Raftery, 1995) in favour of Model 4. A summary of the model's statistics is presented in Table 3. According to the model, WF improved the most in participants whose accuracy in the Before-session was lower, regardless of the stimulation condition. Critically, the planned-contrast test showed that the effect of Group was also significant ( $F(2, 101) = 5.00, p = 0.009$ ). The pairwise contrast comparison showed a significant difference between the IP and CM group only ( $\beta = -0.28, CI = [-0.45 -0.10], t(101) = 3.15, p = .006$  (corrected), Figure 3A); the difference was significant for both Test Area conditions (both  $p < 0.021$ ). Numerically, the difference between the SP and IP groups was approximately half the difference between CM and IP groups, but it did not reach the significance threshold even at the uncorrected level ( $p = 0.15$ ). When tested against zero to establish an absolute rather than a relative change, only CM showed a significant change (increase) in WF ( $\beta = 0.18, CI = [0.06 0.31], t(101) = 2.89, p = .014$  (corrected))

**Table 3. Best-fitting model statistics for the change in Weber Fraction ( $dWF$ ) in the N task. The intercept models CM group in Small Test/Large reference condition; the performance for other groups in the same condition is represented by IP and SP group factors. Statistics for other relevant performance measures, including the average performance across Test Area conditions, were determined using planned-contrast tests and described in the main text and Figure 3B. Statistically significant results are highlighted in grey. Asterisks (\*) mark p-values after Bonferroni-corrections (applicable to group contrasts: CM vs. IP, CM vs. SP, and IP vs. SP).**

<b>N task - Model 4:</b> <b><math>dWF = \text{Group} + \text{TestArea} + \text{Group: TestArea} + \text{base\_WF} + (\text{base\_WF}   \text{Participant})</math></b>					
<b>Predictors</b>	<b>beta</b>	<b>CI (Lower/Upper)</b>		<b>t (df =101)</b>	<b>P-value</b>
Intercept	0.16	0.02	0.30	2.23	0.024
IP group	-0.27	-0.46	-0.07	-2.76	0.020*
SP group	-0.14	-0.33	0.05	-1.46	0.44*
Large Test/Small Reference	0.05	-0.08	0.18	0.73	0.466
WF at baseline	-0.26	-0.39	-0.13	-3.93	< 0.001
IP : Large Test	-0.02	-0.20	0.16	-0.24	1*
SP : Large Test	-0.06	-0.24	0.12	-0.64	1*

Given that the dots' spatial frequency was the task-relevant dimension in the N task, we also assessed whether the WF change in this task was independent from WF change in the D task. We added the WF change and its interaction with group factor as additional factors to the best fitting Model 4. The results showed a negative, but not reliable, association between WF changes in D and N tasks across all groups ( $t(98) = 1.94$ ,  $p = 0.055$ ,  $\beta = -0.23$ ,  $CI = [-0.47 \ 0.01]$ ) and, most critically, no significant group by density WF change interaction ( $F(2, 98) = 0.32$ ,  $p > 0.7$ ), with no effect on the significance of the Group factor. The difference in the BIC criteria = 10.13 in favour of Model 4 indicated that the WF change and its interaction with Group factor in the D task are irrelevant for modelling the WF change in the N task. No association was found if the WF change in the C task and its interaction with Group factor were used in modelling (both  $p > 0.2$ ).

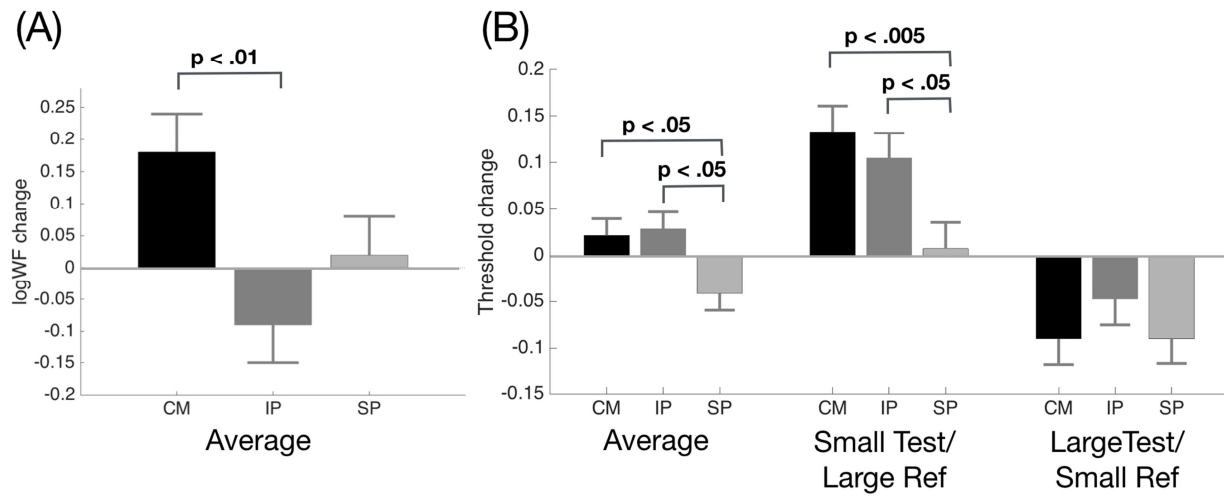


**Figure 3. Effect of stimulation in the N task on (A) WF and (B) Threshold**

### 3.2.2. D and C tasks

Model 3 was best fitting for the D tasks. The model is similar to Model 4, which was best fitting for N task (the difference is only in the random effect), implying a significant association between the WF change and WF magnitude at the baseline ( $\beta = -0.33$ ,  $CI = [-0.45 -0.21]$ ,  $t(101) = -5.52$ ,  $p < 0.001$ ). Model 7 was best fitting for the C task, implying that there was a significant association between the WF and threshold changes ( $\beta = 0.63$ ,  $CI = [0.06 1.20]$ ,  $t(101) = 2.21$ ,  $p = 0.03$ ). No other effect was significant. The effect of Group and its interaction with Test Area were not significant in both cases.

## 3.3. Effect of stimulation on threshold

### 3.3.1. N task

Model 4 was the best-fitting model for the change in threshold in the N task (Table 4), suggesting a significant association between the threshold change and its magnitude at a



baseline. The difference in Bayesian Information Criterion from benchmark Model 1 was equal to 9.42, indicating strong evidence in favour of the best fitting model. Model statistics are shown in Table 3. A significant difference from zero of the intercept and a nearly twice as large beta for Large Test Area (positive and negative, respectively) indicates that there was less bias (symmetrically decreasing for both Test Area conditions) in an estimate of a point of equality between Test and Reference stimuli in the After session (also see Figure 3B). The significant effect of threshold at a baseline indicates that participants who overestimated or underestimated the Test stimulus more in the Before session, showed a greater reduction of their biases, irrespective of the Group factor. Critically, the planned-contrast test showed that the effect of Group was also significant ( $F(2,101) = 4.47$ ,  $p = 0.014$ ). A pairwise group comparison showed that the threshold was differentially affected in the SP group relative to the other groups (Figure 3B; planned contrast of SP vs. CM:  $t(101) = -2.44$ ,  $p = 0.049$ ; planned contrast of SP vs. IP:  $t(101) = -2.71$ ,  $p = 0.024$ ; p-values are Bonferroni-corrected), with no difference between IP and CM groups. This effect however was driven by the difference in Small Test/Large Reference condition (Figure 3B; planned contrast of SP vs. CM:  $t(101) = -3.21$ ,  $p = 0.006$ ; planned contrast of SP vs. IP:  $t(101) = -2.50$ ,  $p = 0.042$ ; Bonferroni-corrected), with no difference between groups in Large Test/Small Reference condition. No significant association was found between the threshold change in the N task and threshold changes in the D task across groups ( $t(98) = 1.73$ ,  $p = 0.087$ ,  $\beta = -0.17$ ,  $CI = [-0.35 \ 0.03]$ ). Critically, the interaction between Group and threshold change in the D tasks was not significant either ( $F(2, 98) = 1.91$ ,  $p = 0.15$ ). The difference in the BIC criteria = 10.24 in favour of Model 4 indicated that the threshold change and its interaction with Group factor in the D task are irrelevant for modelling

the threshold change in the N task. Similarly, no association was found for the corresponding terms in the C task (both  $p > .2$ ).

**Table 4.** Best-fitting model statistics for the change in threshold ( $d$  Threshold) in each task. The interpretation of the model factors is same as in Table 3. Statistically significant results are highlighted in grey. Asterisks (\*) mark p-values after Bonferroni-corrections (where applicable).

<b>N task - Model 4:</b> <b><math>d\text{Threshold} = \text{Group} + \text{TestArea} + \text{Group: TestArea} + \text{base\_Threshold} + (\text{base\_Threshold}   \text{Participant})</math></b>					
Predictors	beta	CI (Lower/Upper)		t (df = 101)	P-value
Intercept	0.13	0.08	0.19	4.83	< 0.001
IP group	-0.03	-0.11	0.05	-0.73	1*
SP group	-0.13	-0.20	-0.05	-3.21	0.005*
Large Test/Small Reference	-0.22	-0.31	-0.14	-5.13	< 0.001
Threshold at baseline	-0.14	-0.26	-0.03	-2.45	0.016
IP : Large Test	0.07	-0.05	0.19	1.19	0.71*
SP : Large Test	0.13	0.01	0.24	2.12	0.11*

### 3.3.2. D and C tasks

Models 4 and 5 were best fitting for the D and C tasks, respectively. The following factors were significant in the D task: intercept ( $\beta = 0.11$ , CI = [0.05 0.17],  $t(101) = 3.69$ ,  $p < 0.001$ ), Large Test Area ( $\beta = -0.25$ , CI = [-0.35 -0.15],  $t(101) = -4.79$ ,  $p < 0.001$ ), and threshold at a baseline ( $\beta = -0.30$ , CI = [-0.47 -0.13],  $t(101) = -3.52$ ,  $p < 0.001$ ). Quantitatively, this across-groups pattern is similar to that observed in the N task. However, considering that at baseline participants showed over-/underestimation pattern opposite to the N task, it implies a greater rather than smaller bias in the estimation of the point of equality between Test and Reference stimuli (also see Figure 1). The effect of the threshold at a baseline indicates that a particularly greater increase is observed in participants who showed a smaller bias in the Before session. Model 5 was best fitting in the C task, but no factor was significant.

### 3.3.3. Analysis of supplementary dataset

Figure 4 shows the results of the analyses of the supplementary dataset, where participants received a sham IP stimulation. WF increased in the After session ( $\beta = 0.16$ , CI = [0.04 0.28],  $t(34) = 2.57$ ,  $p = 0.015$ ). The bias to overestimate and underestimate, respectively, Small Test and Large Test stimuli also decreased in the After session (Small Test:  $\beta = 0.16$ , CI = [0.08 0.24],  $t(34) = 4.12$ ,  $p < 0.001$ ; Large Test:  $\beta = -0.10$ , CI = [-0.18 -0.03],  $t(34) = 2.76$ ,  $p = 0.018$ ). These patterns closely mirror the patterns observed in the CM group of the main experimental data set.

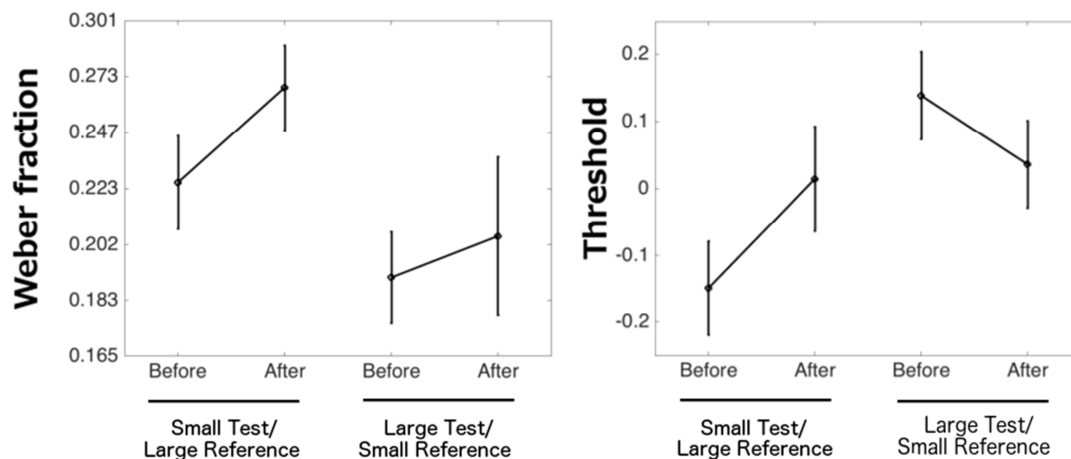


**Figure 4.** Performance in sham-stimulation group of supplementary dataset in the N task. The patterns closely mirror these observed in the CM group of the main experimental data set.

## 4. Discussion

In the present study, transcranial random-noise stimulation (tRNS) was used to understand the mechanisms underlying the visual sense of number (VNS). Firstly, we tested

whether the superior parietal (SP) region, a brain area known for being implicated in numerosity processing (Santens et al., 2010), hosts a numerosity code (i.e. whether it has a representational role), or whether instead it modulates weights for stimulus features, which could be used for the numerosity extraction (i.e. a modulatory role). We predicted that stimulation may affect the VNS precision if the SP role is representational, and may affect the threshold (contrast gain) if its role were instead modulatory. Secondly, we tested whether the intraparietal (IP) regions represent a numerosity ‘read-out’ independent of continuous magnitudes or whether their metrics overlap. In the former case, IP stimulation may affect the VNS precision independently of continuous magnitude judgements.

Our results can be summarised as follows. Firstly, SP stimulation in the numerosity task induced a contrast gain, which significantly differed from a contrast gain following both IP- and motor-tRNS. The results are consistent with the hypotheses of a modulatory role of the SP in the VNS. Secondly, we observed an improvement in VNS precision following IP stimulation relative to stimulation of the control motor regions, which was statistically independent of the changes in the precision of continuous magnitude judgements, suggesting that the IP implements numerical code independently of the continuous magnitude features, at least the one used in the current study.

The lack of contrast gain following SP stimulation in the density and coherence tasks, especially in the density task, allows for a better understanding of the role of the superior parietal region in the VNS. Dot density in the test stimulus was the only varying feature in both density and numerosity tasks. It is well documented that stimulus change or novelty is a sufficient factor to capture attention (Corbetta & Shulman, 2002; Vossel, Weidner, Thiel, & Fink,

2009), and such bottom-up attentional modulation may result in a signal gain, “effective contrast” (Kastner & Ungerleider, 2001; Keitel, Andersen, Quigley, & Muller, 2012; Carrasco, Ling, & Read, 2004). If the SP was implicated in this process by providing a contrast boost to a stimulus with varying features (i.e., dot density), then an increased excitability in this region should have also resulted in a similar effect in the density task. In other words, stimulation would simply increase a bias towards selecting a stimulus with more varying features without implicating weighting of continuous magnitude features. Instead, in our study we observed a bias towards overestimating the test stimulus only in the task where a magnitude was determined by a combination of features. Its behavioural manifestation was that it countered a generic trend towards a reduction of numerosity overestimation for varying stimuli with a dense dot composition, i.e., Small Test stimuli. The lack/statistical independence of a similar effect in the coherence task is also informative. Whereas this task featured a two-dimensional magnitude structure (similarly to the numerosity task, random-deterministic as compared to area-density), the size of the stimulus cloud in the coherence task bore no direct relation to its magnitudes. This suggests that the SP is engaged if a selection of features relevant for magnitude estimation is required. This is in line with the proposed role of the superior parietal lobule as a priority map of dorsal attentional network, implementing selective attention and exerting top-down control on the bottom-up visual stream implemented in the ventral attentional network (Corbetta & Shulman, 2002; Bisley & Goldberg, 2010).

Our study complements previous findings of improvement in the VNS following intraparietal tRNS (e.g., Cappelletti et al., 2013) and extends them in an important way. Here we show that modulatory effect occurs following a one-session stimulation suggesting a utility

of tRNS as a tool for probing cognitive mechanisms with the goal of their better understanding. We also show a performance modulation in a larger numerosity range than previously studied. This is important as it has been suggested that the codes for large numerosity may differ not only from the codes for numbers in the subitising range (Kaufman, Lord, Reese, & Volkman, 1949), but also from codes for relatively small numerosities outside the subitising range. Anobile et al. (Anobile, Cicchini, & Burr, 2014) proposed that extracting large numerosities may rely on spatial frequency of stimulus items whereas small numerosity may be accessed by the visual system directly. Whereas the processing routes for small and large numerosities may still differ, our results in combination with results by Cappelletti et al. (2013) suggest that their codes may converge at the level of the IP region.

Not all the stimulation effects however were specific in the current study. Although IP stimulation resulted in an improvement of performance compared to the stimulation of motor regions, the effect was not statistically different from (albeit numerically greater than) the effect of the SP stimulation. In other words, we observed a differential effect of SP stimulation on the threshold but not a differential effect of IP stimulation on the precision. Moreover, we did not observe a WF improvement in absolute terms. Whereas the control group showed a significant increase of WF if tested against zero, a decrease of WF in the IP group did not reach significance.

These results may hallmark a limitation of the present study as it could be argued that the control group stimulation does not represent a true baseline and produces an unexpected region-specific “contamination” effect, impairing the performance. This interpretation is however unlikely for several reasons. Firstly, the analysis of the supplementary dataset

demonstrated that performance changes between the Before and After sessions in participants who received a sham stimulation are essentially the same to those observed in the CM group. Even though the two datasets are not directly comparable because of some differences in the study protocols, the mixed-effect modelling produced very similar estimates of how the performance changed. Secondly, we implemented a very stringent task-based control for the stimulation effects. The analytical procedures demonstrated that the stimulation-dependent WF changes were task-specific, whereas neither motor areas, which provided an anatomical control condition, nor its circuitry are known to be involved in any specialised cognitive processing of visual magnitudes. It is still of course possible that non-specific stimulation effects may elicit task-specific effects through an interaction with some generic task properties, e.g., task difficulty. However, this is unlikely because the control tasks were either easier or more difficult than the numerosity task, as it is suggested by Weber Fraction data in Figure 1. Finally, a possible contamination effect is not fully supported by the data as no differentiation between SP and IP stimulation effects on WF was concomitant with no differentiation between SP and CM stimulation. Assuming that this pattern is a consequence of a “dose-dependent” stimulation effect, then it is more likely to occur for the spatially and functionally proximal IP and SP sites than for the (spatially and functionally) distant CM and SP sites. Moreover, a study on alternate current stimulation suggests that it may be easier for the electrical current to reach brain areas situated inside sulci compared to lateral parts of a gyrus (Kanai, Chaieb, Antal, Walsh, & Paulus, 2008). This study has shown that stimulation of V1 elicited phosphemes in a visual field associated with regions residing deeply in the calcarine sulcus, not with a lateral part of the V1. Relating these findings to the current study, it is possible that the regions within intraparietal

sulcus might still receive some stimulation when the targeted region was the SP area but not the opposite; that is, the SP stimulation may also affect the IP, whereas the IP stimulation did not significantly affect lateral SP cortex.

Taken together, our results highlight the importance of higher-order integrative processes in the VNS, mediated by the SP, and are in good agreement with a computational model advanced by Stoianov and Zorzi (2012) showing that numerosity is an emergent property based on continuous magnitude statistics. Unlike earlier computational models of enumeration, which assumed that continuous magnitudes confound numerosity (Dehaene & Changeux, 1993; Verguts & Fias, 2004), the model by Stoianov and Zorzi contains a hidden layer that codes continuous magnitudes and the output layer that implements their weighted integration. It remains an open question whether the first abstract 'read-out' is provided in a form of summation, as in their model, or as a number-selective coding. It has previously been argued (Karolis & Butterworth, 2016; Stoianov & Zorzi, 2012) that an abstract representation in a form of number-selective code is likely to require an accumulator process preceding it.

Some researchers however argue against the existence of an abstract numerosity code. For instance, Dakin and colleagues proposed a computational model based on a unified mechanism for density and numerosity extraction - the outputs of high and low frequency visual filters (Dakin et al, 2011). The model accounts well for the overestimation of density and numerosity of stimuli with a large area, as reported in their study. However, this type of overestimation, which is the premise Dakin et al.'s model is built on, is not validated in a considerably larger sample of naïve participants assessed in the current study. The pattern is only replicated in the density task, but it is reversed in the numerosity task (see Table 1).



The current study is consistent with the ANS model in that the VNS is characterised as a multi-stage process. Since several studies showed a positive association between the VNS and mathematical competence (Halberda, Mazocco, & Feigenson, 2008; Tibber et al., 2013), it is important to clarify at which processing stage this association emerges. One study (Tibber et al., 2013) suggests that the association is not unique for the VNS, and other visuospatial abilities may also correlate with math achievements. However, the same study also demonstrates that precision of numerosity is a better predictor than precision in a spatial frequency task, indicating that processes implicated in the VNS above and beyond the spatial frequency processing may contribute to strengthening the association. One could speculate that the ability to integrate information across several visuospatial dimensions may be important for developing a better mathematical competence in addition to generic visuospatial abilities.

Lastly, a limitation of the present study should be acknowledged. Even though the observed differential effects of stimulation were specific in terms of their spatial resolution, their exact anatomical localisation remains undetermined. To differentiate the two, we have distinguished between the terms 'SPL' and 'IPS', referring to the anatomically defined regions, and 'SP' and 'IP', referring to the loci of stimulations in the present study. However, it is important to note that the issue of finding an exact anatomical underpinning for the VNS is largely orthogonal to the main purpose of this study. Previous fMRI studies have achieved a considerable progress in this respect. The current study therefore complements previous (correlation-based) fMRI studies and contributes to a better understanding of the VNS mechanisms.

## Conclusions

This study showed that the VNS is a process of statistical inference based on continuous magnitude features. In this process, the superior parietal areas play a role in weighing stimulus feature, whereas the intraparietal region contains an abstract 'read-out' of numerosity. This suggests that the independence of numerosity representation from continuous magnitudes refers only to the final stages of the process of numerosity extraction.

**Acknowledgments**

This research was supported by the Tomsk State University grant 8.1.09.2017

ACCEPTED MANUSCRIPT

**References:**

- Anobile, G., Cicchini, G. M., & Burr, D. C. (2014). Separate Mechanisms for Perception of Numerosity and Density. *Psychological Science*, 25(1), 265-270. doi: 10.1177/0956797613501520
- Bisley, J. W., & Goldberg, M. E. (2010). Attention, Intention, and Priority in the Parietal Lobe. *Annual Review of Neuroscience*, Vol 33, 33, 1-21. doi: 10.1146/annurev-neuro-060909-152823
- Bressler, S.L., & Menon, V. (2010). Large-scale brain networks in cognition: emerging methods and principles. *Trends in Cognitive Sciences*, 14, 277–290. doi:10.1016/j.tics.2010.04.004
- Brezis, N., Bronfman, Z. Z., Jacoby, N., Lavidor, M., & Usher, M. (2016). Transcranial Direct Current Stimulation over the Parietal Cortex Improves Approximate Numerical Averaging. *Journal of Cognitive Neuroscience*, 28(11), 1700-1713. doi: 10.1162/jocn\_a\_00991
- Cappelletti, M., Gessaroli, E., Hithersay, R., Mitolo, M., Didino, D., Kanai, R., Cohen Kadosh, R., & Walsh, V. (2013). Transfer of Cognitive Training across Magnitude Dimensions Achieved with Concurrent Brain Stimulation of the Parietal Lobe. *Journal of Cognitive Neuroscience*, 173-173.
- Carrasco, M., Ling, S., & Read, S. (2004). Attention alters appearance. *Nature Neuroscience* 7, 308–313. doi:10.1038/nn1194
- Chaieb, L., Antal, A., & Paulus, W. (2015). Transcranial random noise stimulation-induced plasticity is NMDA-receptor independent but sodium-channel blocker and benzodiazepines sensitive. *Front Neurosci*, 9, 125. doi:10.3389/fnins.2015.00125

- Corbetta, M., & Shulman, G. L. (2002). Control of goal-directed and stimulus-driven attention in the brain. *Nature Reviews Neuroscience*, 3(3), 201-215. doi: 10.1038/nrn755
- Dakin, S. C., Tibber, M. S., Greenwood, J. A., Kingdom, F. A. A., & Morgan, M. J. (2011). A common visual metric for approximate number and density. *Proceedings of the National Academy of Sciences of the United States of America*, 108(49), 19552-19557. doi: 10.1073/pnas.1113195108
- Davidse, N. J., de Jong, M. T., Shaul, S., & Bus, A. G. (2014). A twin-case study of developmental number sense impairment. *Cognitive Neuropsychology*, 31(3), 221-236. doi: 10.1080/02643294.2013.876980
- Dehaene, S., & Changeux, J. P. (1993). Development of Elementary Numerical Abilities - a Neuronal Model. *Journal of Cognitive Neuroscience*, 5(4), 390-407. doi: 10.1162/Jocn.1993.5.4.390
- Dehaene, S., Izard, V., Spelke, E., & Pica, P. (2008). Log or linear? Distinct intuitions of the number scale in western and amazonian indigene cultures. *Science*, 320(5880), 1217-1220. doi: 10.1126/science.1156540
- DeWind, N. K., & Brannon, E. M. (2012). Malleability of the approximate number system: effects of feedback and training. *Frontiers in Human Neuroscience*, 6. doi: 10.3389/Fnhum.2012.00068
- Frond, I., Haenel, N. V., & Wichmann, F. A. (2011). Inference for psychometric functions in the presence of nonstationary behavior. *J Vis*, 11(6). doi: 10.1167/11.6.16

- Gebuis, T., Kadosh, R. C., & Gevers, W. (2016). Sensory-integration system rather than approximate number system underlies numerosity processing: A critical review. *Acta Psychologica*, 171, 17-35. doi: 10.1016/j.actpsy.2016.09.003
- Gebuis, T., & Reynvoet, B. (2012). The Interplay Between Nonsymbolic Number and Its Continuous Visual Properties. *Journal of Experimental Psychology-General*, 141(4), 642-648. doi: 10.1037/a0026218
- Halberda, J., & Feigenson, L. (2008). Developmental change in the acuity of the "Number sense": The approximate number system in 3-, 4-, 5-, and 6-year-olds and adults. *Developmental Psychology*, 44(5), 1457-1465. doi: 10.1037/a0012682
- Halberda, J., Mazocco, M. M. M., & Feigenson, L. (2008). Individual differences in non-verbal number acuity correlate with maths achievement. *Nature*, 455(7213), 665-U662. doi: 10.1038/nature07246
- Harvey, B. M., Klein, B. P., Petridou, N., & Dumoulin, S. O. (2013). Topographic Representation of Numerosity in the Human Parietal Cortex. *Science*, 341(6150), 1123-1126. doi: 10.1126/science.1239052
- Iuculano, T., Tang, J., Hall, C. W. B., & Butterworth, B. (2008). Core information processing deficits in developmental dyscalculia and low numeracy. *Developmental Science*, 11(5), 669-680. doi: 10.1111/j.1467-7687.2008.00716.x
- Jordan, N. C., Glutting, J., & Ramineni, C. (2010). The importance of number sense to mathematics achievement in first and third grades. *Learning and Individual Differences*, 20(2), 82-88. doi: 10.1016/j.lindif.2009.07.004

- Kanai, R., Chaieb, L., Antal, A., Walsh, V., & Paulus, W. (2008). Frequency-Dependent Electrical Stimulation of the Visual Cortex. *Current Biology*, 18(23), 1839-1843. doi: 10.1016/j.cub.2008.10.027
- Karolis, V., & Butterworth, B. (2016). What counts in estimation? The nature of the preverbal system. *Prog Brain Res*, 227, 29-51. doi: 10.1016/bs.pbr.2016.04.025
- Kass, R. E., & Raftery, A. E. (1995). Bayes Factors. *Journal of the American Statistical Association*, 90(430), 773-795. doi: 10.1080/01621459.1995.10476572
- Kastner, S., & Ungerleider, L. G. (2001). The neural basis of biased competition in human visual cortex. *Neuropsychologia*, 39(12), 1263-1276. doi: Doi 10.1016/S0028-3932(01)00116-6
- Kaufman, E. L., Lord, M. W., Reese, T. W., & Volkman J. (1949). The Discrimination of visual number. *The American Journal of Psychology*, 62(4), 498-525.
- Keitel, C., Andersen, S. K., Quigley, C., & Muller, M. M. (2012). Attentional gain control and competitive interactions influence visual stimulus processing independently. *Perception*, 41, 128-128.
- Koyama, M., Hasegawa, I., Osada, T., Adachi, Y., Nakahara, K., & Miyashita, Y. (2004). Functional magnetic resonance imaging of macaque monkeys performing visually guided saccade tasks: Comparison of cortical eye fields with humans. *Neuron*, 41(5), 795-807. doi: Doi 10.1016/S0896-6273(04)00047-9
- Lambrechts, A., Karolis, V., Garcia, S., Obende, J., & Cappelletti, M. (2013). Age does not count: resilience of quantity processing in healthy ageing. *Frontiers in Psychology*, 4. doi: Artn 865 10.3389/Fpsyg.2013.00865

- Nieder, A. (2016). The neuronal code for number. *Nature Reviews Neuroscience*, 17(6), 366-382. doi: 10.1038/nrn.2016.40
- Nieder, A., Freedman, D. J., & Miller, E. K. (2002). Representation of the quantity of visual items in the primate prefrontal cortex. *Science*, 297(5587), 1708-1711. doi: Doi 10.1126/Science.1072493
- Nieder, A., & Miller, E. K. (2004). A parieto-frontal network for visual numerical information in the monkey. *Proceedings of the National Academy of Sciences of the United States of America*, 101(19), 7457-7462. doi: 10.1073/pnas.0402239101
- Piazza, M., Izard, V., Pinel, P., Le Bihan, D., & Dehaene, S. (2004). Tuning curves for approximate numerosity in the human intraparietal sulcus. *Neuron*, 44(3), 547-555. doi: Doi 10.1016/J.Neuron.2004.10.014
- Piazza, M., Facoetti, A., Trussardi, A. N., Berteletti, I., Conte, S., Lucangeli, D., Dehaene, S., & Marco Zorzi. (2010). Developmental trajectory of number acuity reveals a severe impairment in developmental dyscalculia. *Cognition*, 116(1), 33-41. doi.org/10.1016/j.cognition.2010.03.012
- Pinel, P., Piazza, M., Le Bihan, D., & Dehaene, S. (2004). Distributed and overlapping cerebral representations of number, size, and luminance during comparative judgments. *Neuron*, 41(6), 983-993. doi: Doi 10.1016/S0896-6273(04)00107-2
- Polania, R., Paulus, W., Antal, A., & Nitsche, M. A. (2011). Introducing graph theory to track for neuroplastic alterations in the resting human brain: A transcranial direct current stimulation study. *NeuroImage*, 54, 2287-2296. doi: doi.org/10.1016/j.neuroimage.2010.09.085



- Reynolds, J. H., & Heeger, D. J. (2009). The Normalization Model of Attention. *Neuron*, 61(2), 168-185. doi: 10.1016/j.neuron.2009.01.002
- Roitman, J. D., Brannon, E. M., & Platt, M. L. (2007). Monotonic coding of numerosity in macaque lateral intraparietal area. *Plos Biology*, 5(8), 1672-1682. doi: ARTN e208 10.1371/journal.pbio.0050208
- Roitman, J. D., Brannon, E. M., & Platt, M. L. (2012). Representation of numerosity in posterior parietal cortex. *Front Integr Neurosci*, 6, 25. doi: 10.3389/fnint.2012.00025
- Roitman, J. D., & Shadlen, M. N. (2002). Response of neurons in the lateral intraparietal area during a combined visual discrimination reaction time task. *Journal of Neuroscience*, 22(21), 9475-9489.
- Santens, S., Roggeman, C., Fias, W., & Verguts, T. (2010). Number Processing Pathways in Human Parietal Cortex. *Cerebral Cortex*, 20(1), 77-88. doi: 10.1093/cercor/bhp080
- Sereno, M. I., Pitzalis, S., & Martinez, A. (2001). Mapping of contralateral space in retinotopic coordinates by a parietal cortical area in humans. *Science*, 294(5545), 1350-1354. doi: Doi 10.1126/Science.1063695
- Stoianov, I., & Zorzi, M. (2012). Emergence of a 'visual number sense' in hierarchical generative models. *Nature Neuroscience*, 15(2), 194-196. doi: 10.1038/nn.2996
- Terney, D., Chaieb, L., Moliadze, V., Antal, A., & Paulus, W. (2008). Increasing Human Brain Excitability by Transcranial High-Frequency Random Noise Stimulation. *Journal of Neuroscience*, 28(52), 14147-14155. doi.org/10.1523/JNEUROSCI.4248-08.2008

- Tibber, M. S., Greenwood, J. A., & Dakin, S. C. (2012). Number and density discrimination rely on a common metric: Similar psychophysical effects of size, contrast, and divided attention. *Journal of Vision*, 12(6). doi: Artn 810.1167/12.6.8
- Tibber, M. S., Manasseh, G. S. L., Clarke, R. C., Gagin, G., Swanbeck, S. N., Butterworth, B., Lotto, R.B., & Dakin, S. C. (2013). Sensitivity to numerosity is not a unique visuospatial psychophysical predictor of mathematical ability. *Vision Research*, 89, 1-9. doi: 10.1016/j.visres.2013.06.006
- van der Groen, O. & Wenderoth, N. (2016). Transcranial random noise stimulation of visual cortex: stochastic resonance enhances central mechanisms of perception. *Journal of Neuroscience*, 36, 5289–5298. doi: 10.1523/JNEUROSCI.4519-15.2016
- Verguts, T., & Fias, W. (2004). Representation of number in animals and humans: A neural model. *Journal of Cognitive Neuroscience*, 16(9), 1493-1504. doi: Doi 10.1162/0898929042568497
- Vossel, S., Weidner, R., Thiel, C. M., & Fink, G. R. (2009). What is "Odd" in Posner's Location-cueing Paradigm? Neural Responses to Unexpected Location and Feature Changes Compared. *Journal of Cognitive Neuroscience*, 21(1), 30-41. doi: Doi 10.1162/Jocn.2009.21003
- Walsh, V. (2003). A theory of magnitude: common cortical metrics of time, space and quantity. *Trends in Cognitive Sciences*, 7(11), 483-488. doi: 10.1016/j.tics.2003.09.002
- Wassermann, E. M. (1998). Risk and safety of repetitive transcranial magnetic stimulation: report and suggested guidelines from the international workshop on the safety of repetitive transcranial magnetic stimulation, June 5-7, 1996. *Evoked Potentials-*

Electroencephalography and Clinical Neurophysiology, 108(1), 1-16. doi: Doi 10.1016/S0168-5597(97)00096-8

Wilkinson, G. N., & Rogers, C. E. (1973). Symbolic Description of Factorial Models for Analysis of Variance. The Royal Statistical Society Series C-Applied Statistics, 22(3), 392-399.